INVESTIGATION OF LOW-COST 3D BIOPRINTING PLATFORMS FOR CONSTRUCTING TISSUE SCAFFOLDS

By

ROBERT THOMAS WARREN

A thesis submitted to the

School of Graduate Studies

Rutgers, The State University of New Jersey

In partial fulfillment of the requirements

For the degree of

Master of Science

Graduate Program in Biomedical Engineering

Written under the direction of

Joseph Freeman, Ph.D.

And approved by

_____

_____

_____

New Brunswick, New Jersey

MAY, 2019

ABSTRACT OF THE THESIS

Title

By ROBERT THOMAS WARREN

Thesis Director:

Joseph Freeman, Ph.D.

Fabricating multiphase biomaterials using bioprinting is expensive, preventing academic institutions and startup companies from using these materials more frequently in their research. By introducing a low-cost bioprinting alternatives, we can lower the cost of entry into the field. In this study we assess the feasibility of converting a thermoplastic 3D printer into a low-cost dual head 3D bioprinter capable of printing thermoplastics and bioinks along with building a low-cost pneumatic pressure driven triple head 3D bioprinter. We also demonstrate and characterize the dual head 3D bioprinter's ability to fabricate a variety of complex tissue scaffolds from commonly used biomaterials such as polyethylene glycol diacrylate (PEGDA) hydrogels and polycaprolactone (PCL) thermoplastic filament.

DEDICATION

Mom, Dad, Sabrina, Jess, you may never read past this page and I wouldn't blame you.

ACKNOWLEDGEMENTS

First and foremost, Dr. Joseph Freeman for his support over the past 4 years starting from my junior year of undergraduate engineering all the way to the end of my Masters. Without his guidance I would not be where I am today. Dr. Ronke Olabisi for her willingness to aide me both academically and professionally, NASA! Dr. Jay Sy for providing valuable input and agreeing to be a part of my committee. Dr. Gormley lab for analyzing our PCL filament molecular properties. Dr. Shreiber lab for allowing us to use their rheometer to analyze our hydrogel viscosity. Gabriel Valdez and Steve Hermida for their assistance with constructing the triple-head bioprinter. My good friend Patrick Bargoud for helping me draw the circuit for my 3D printer to Arduino communication system. Lastly, I would like to thank my friends from the BME department who made going to the lab a fun environment; especially Christian, Mike, Tim, Mary Pat, and Fernando. Also special thanks to my friend Rachel Hughes!

TABLE OF CONTENTS

LIST OF TABLES

LIST OF ILLUSTRATIONS

CHAPTER 1: BACKGROUND AND INTRODUCTION

1.1. Overview of the field of Bioprinting

Millions of people around the world suffer from tissue and organ damage due to congenital defects, trauma, and disease. As of June 2017, according to the U.S. Department of Health & Human Services, nearly 120,000 patients are in critical need of an organ transplant in the United States alone [1]. It is the goal for tissue engineering to replace human tissues which are diseased or damaged [2-4]. On demand tissue and organ replacement is highly sought after and the success of tissue engineering would have a global impact. 3D bioprinting, a branch of tissue engineering that has the capabilities to fabricate complex 3D tissue constructs, patterned from multiple types of biomaterials, that can provide a functionally in vitro environment for cell growth [5, 6]. Scaffolds are a type of tissue construct that are commonly used in tissue engineering which are typically made out of different polymeric biomaterials [7]. Scaffolds are used extensively in tissue engineering as a support structure for cells to proliferate and differentiate on. 3D bioprinting is an attractive alternative for fabricating tissue scaffolds as it offers the ability to accurately control scaffold structure and cell deposition with high accuracy and precision [1, 8].

Biomedical applications of additive manufacturing (AM) are advancing rapidly and are capable of fulfilling the limitations of biocompatibility, reproducibility seen in other tissue manufacturing methods [2]. Crucial to this is the precise control the user has over the product's construction and material properties. AM techniques employ an automated process of depositing materials in layers to construct three-dimensional objects

from specially made computer-aided designs. The ability to create biological structures accurately and precisely has led to the emergence of bioprinters as a promising tool for performing in vitro 2D cell culture studies, drug delivery, the fabrication of biomaterial scaffolds for tissue engineering [9-11]. AM also allows for the easy incorporation of computer-aided design (CAD) software, which allows users to load the CAD file into the printing system and automatically fabricate the structure [12].

Previous studies have demonstrated the ability of hydrogels to serve as a highly functional extracellular matrix for cell growth [13]. In addition, biocompatible electroactive polymers have been studied for use as biosensors, artificial muscles, and other applications [14]. When swelled in an ionic solution and place in an electric field, the hydrogel experiences a bending movement as result of the shifting of ions and water molecules. In an attempt to test the printability of electroactive polymers, we use an established formulation consisting of poly(ethylene glycol) diacrylate (PEGDA) and poly(acrylic acid) (PAA) [15].

Currently, high-end bioprinters on the market can cost anywhere between $8,000 to $200,000 [16, 17]. The cost of entering the bioprinting field is very high which inhibits academic institutions and smaller corporations from participating in the field. The systems we developed present cheap and functional alternatives to current commercially available bioprinters. Because of the severe limitations imposed by a high cost of entry into the field of bioprinting, there exists a need for a novel bioprinting system that can provide a high level of accuracy, is cost effective, and can fabricate functional and complex tissue scaffolds.

It is our aim to present highly affordable yet functional bioprinting platforms for all consumers. This thesis is broken into two projects. The first being the design and analysis of a linear actuator modification that can convert a low-cost dual head 3D printer into a 3D bioprinter that is capable of depositing both thermoplastics and bioinks. Additionally, we characterized the printer's performance and fabricated scaffold properties. The second project describes the design for constructing a low-cost pneumatic pressure driven triple head 3D bioprinter that can deposit one thermoplastic and two bioinks.

CHAPTER 2: THE DEVELOPMENT OF A LOW-COST DUAL HEAD 3D BIOPRINTER

2.1. Introduction

Although there are many different additive manufacturing mechanisms for bioprinting, the most common and affordable technique is microextrusion [18, 19]. Microextrusion offers the advantage of dispensing various types and viscosities of biomaterials while also offering ease of use and scalability [16, 20]. Between the two different microextrusion based techniques, pneumatic and mechanical, we chose to employ a mechanical screw extrusion system. The greater spatial control and ability to dispense higher viscosity bioinks made it an attractive solution [16]. This technology has been adopted into many other areas of biomedical research such as pharmaceutics for drug testing, cancer research, and tissue engineering [20]. Microextrusion is a fast and controllable deposition method allowing for short print time and is also capable of generating 3D tissue constructs of various anatomical sizes and shapes.

In this chapter we present a 3D printable microextrusion device and related software that can convert a commercial low-cost 3D printer into a 3D bioprinter that can print bioinks alongside thermoplastics. We apply this printer to the field of tissue engineering where we fabricate muscle scaffolds and demonstrate the printer's ability to produce complex structures. We employ a widely used bioprinting method involving bioink deposition, ultraviolet light cross-linking, and computer controlled printing [21].

2.2. Materials and Methods

2.2.1. MakerBot Replicator Original Dual

The 3D printer used for this study was a MakerBot Replicator Original Dual (MakerBot Industries, USA). The system has a listed 22.5 x 14.5 x 15 cm build volume, 40 mm/s print speed, and print resolutions 11 μm precision for both x and y axes. The printer is running Sailfish FlashForge Creator X, version v7.7. The high intensity ultraviolet used for this study was a Blak-Ray B-100A Longwave Ultravoilet Lamp (UVP, USA). The needle tips used for this study were an 18 to 22 gauge tips (Howard Electronics Instruments Inc., USA)

2.2.2. CAD modifications, use of linear actuator

With the aim of making 3D bioprinters more readily available, we have created a 3D printable microextrusion device that can be outfitted to an open-source thermoplastic-based 3D printer. The microextrusion device is a linear actuator that is designed to fit a common 3D printer stepper motor. We used computer-aided-design (CAD) software to design the microextrusion device and printed the components on an Ultimaker 2+ using

PLA or ABS. The device is designed to replace one of the two thermoplastic extruding stepper motors on a dual extruding printer. We based our device off the design described by Hinton et al. The stepper motor used in this study was a Moon's Industries stepper motor When in motion, the microextrusion device compresses a 1 mL or 5 mL syringe at a rate determined by the stepper motor. G-code manipulation of print files were necessary to correct the stepper motor rotation speeds as to allow for proper bioink deposition.

The linear actuator consisted of the stepper motor oriented in a vertical position with 3D printed components mounted to the motor. The components consist of a base, driving screw, drive plate, walls, and top plate, Figure 1. The shaft of the stepper motor was connected to a screw via a flexible coupling. When functioning, the stepper motor spins in a counter clockwise manner causing the drive plate to lower which subsequently compresses loaded syringes resulting in bioink extrusion.

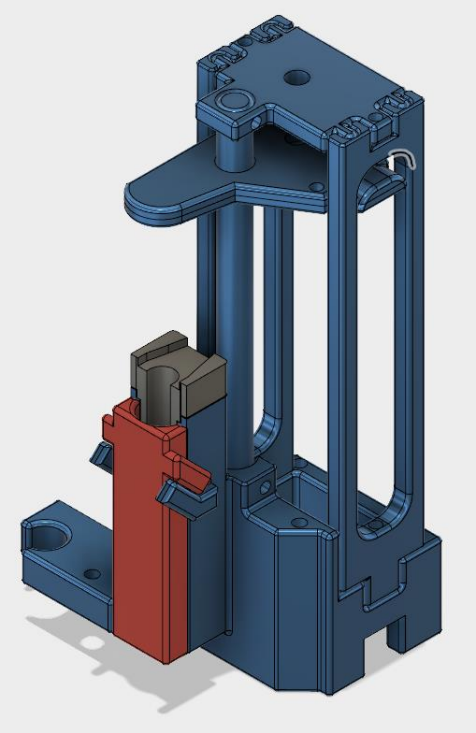

Figure 1 - Linear Actuator

2.2.3. Python Parsing Program

A major issue when attempting to print bioinks was the slow rotational speed of the stepper motor controlling the stepper motor controlling the microextrusion device. This slow rotation rate resulted in an inadequate amount of compression force applied to the syringe. MakerBot Desktop, the program used to slice STL files for this study, is designed to for printing thermoplastic materials, not bioinks. This problem can be visualized by slicing an STL file with and analyzing the resulting G-code. The difference between the two values displayed in the red boxes determines the amount of material extruded in units of mm, refer to Figure 2. In this example, 17.043 - 11.7465 = 5.2965, results in 5.2965 mm of filament extruded. The amount of filament extruded directly

correlates to the rotation rate of the stepper motor. In order to increase the rotation rate of the stepper motor, the amount of material extruded had to be increased significantly.

```
G1 X93.750 Y17.600 Z0.600 F0; Retract
G1 X93.750 Y17.600 Z0.600 F3000; Retract
G1 X94.950 Y18.800 Z0.600 F9000; Travel Move
G1 X94.950 Y41.200 Z0.600 F5400 A11.7465; Inset
G1 X105.050 Y41.200 Z0.600 F5400 A17.043; Inset
G1 X105.050 Y18.800 Z0.600 F5400 A28.7895; Inset
M73 P41; Update Progress
G1 X94.950 Y18.800 Z0.600 F5400 A34.08585; Inset
G1 X94.950 Y18.800 Z0.600 F0; Retract
G1 X94.950 Y18.800 Z0.600 F3000; Retract
G1 X94.550 Y18.400 Z0.600 F9000; Travel Move
G1 X94.550 Y41.600 Z0.600 F2400 A46.2519; Inset
M73 P42; Update Progress
G1 X105.450 Y41.600 Z0.600 F2400 A51.96795; Inset
M73 P43; Update Progress
G1 X105.450 Y18.400 Z0.600 F2400 A64.134; Inset
M73 P44; Update Progress
G1 X94.550 Y18.400 Z0.600 F2400 A69.8499; Inset
M73 P45; Update Progress
G1 X94.550 Y18.400 Z0.600 F0; Retract
G1 X94.550 Y18.400 Z0.600 F3000; Retract
G1 X95.236 Y19.349 Z0.600 F9000; Travel Move
G1 X104.764 Y28.877 Z0.600 F10200 A76.91595; Infi
```

Figure 2 - G-code sliced by default settings

The solution to this problem was to design a Python program that could parse through the G-code and increase these filament extrusion value. This in turn would result in a greater amount of material to be deposited and a faster rotation rate for the stepper motor. See the figures below for the code of the parsing program.

```
file = 'imbed'#input('Enter your gcode filename (w/o extension):')
file_txt = file + '.gcode'
file_change = file + '-change.txt'
file_same = file + '-same.txt'


print(file_change + ' file created...')
print(file_same + ' file created...')
# ----------------------------------------------------------------
# reads input text document and splits the file into change and same files
with open(file_txt,'r') as rf:
    with open(file_same, 'w') as wf_same, open(file_change,'w') as wf_change:
        size_to_read = 1
        rf_contents = rf.read(size_to_read)
        #print(rf_contents)
        M = 0 #on/off switch
        token = []
        token2= ''
        while len(rf_contents) > 0:
            if (token == ['M', '1', '3', '5', ' ', 'T', '0']):
                M = 1
                wf_same.write('* ')
            if (token == ['M', '1', '3', '5', ' ', 'T', '1']):
                M = 0
            if(M==1):
                wf_change.write(rf_contents)
            if (M == 0):
                wf_same.write(rf_contents)
                #wf_same.write('*')
                M = 0
            token.append(rf_contents)
            if (len(token) == 8):
                del token[0]
            #print(token)
            rf_contents = rf.read(size_to_read)
```

Figure 3 - G-code Parser, identification and token system

In the first part of the program shown in Figure 3, the user can identify the specific G-code file they would like to parse for bioprinting. The program then uses a token system in order to identify portions in the G-code that need to be changed for bioprinting. Two tokens are required because this system is a dual extruder printer and there will be two different sections within G-code. One section will be the bioink printing

which is controlled by the linear actuator, the other section controls the default thermoplastic printing. It was imperative that the thermoplastic printing section was not modified.

```
# convert change and same text files to strings
with open(file_change,'r') as wf_change, open(file_same, 'r') as wf_same:
    wf_change_c = wf_change.read(size_to_read)
    wf_same_c = wf_same.read(size_to_read)
    wf_same_Str = ''
    wf_change_Str = ''

    while len(wf_same_c) > 0:
        #print(wf_same_c)
        wf_same_Str = wf_same_Str + wf_same_c
        wf_same_c = wf_same.read(size_to_read)
    #print(wf_same_Str)

    while len(wf_change_c) > 0:
        wf_change_Str = wf_change_Str + wf_change_c
        wf_change_c = wf_change.read(size_to_read)
    #print(wf_change_Str)

# ------------------------------------------------------------------
# find of '; End of print' and save for insertion at end

if wf_change_Str.find('; End of print') != -1:
    x = wf_change_Str.find('; End of print')
    end = wf_change_Str[x:]
if wf_same_Str.find('; End of print') != -1:
    x = wf_same_Str.find('; End of print')
    end = wf_same_Str[x:]
```

Figure 4 - G-code Parser, string manipulation

```
i = 0
indexA = 0
valueA = 0
incrementA =15
n = 5 #n digits to the right of the decimal point
new_c_str = ''
# retrieve values after A and convert them from strings to floats
test_str = ''
test_float = 0
```

Figure 5 - G-code Parser, multiplier definition

The second section shown in Figure 4 displays the string manipulation required to read the original G-code and translate it into a new G-code file. In addition to the new G-code file, files labelled as “change” and “same” are also created. These files record the state of the parsing process at crucial steps so that if something were to go wrong in the final code, the problem could be identified more easily by using the “change” and “same” files. Figure 5 shows the definition of the multiplier value. The extrusion values will be increased by this multiplier in order to increase the stepper motor’s rotation rate.

```
while i < len(wf_change_Str):
    # --------------- Skipping retract distance  -----------------
    if wf_change_Str[i] == 'A' and wf_change_Str[i+1] == '0':
        indexA = i
     # --------------- ends in space --------------------
    if wf_change_Str[i] == 'A' and wf_change_Str[i+1] != '0' \
            and wf_change_Str[i+1:i+4] != '127'\
            and wf_change_Str[i+1:i+6] != 'ctive'\
            and wf_change_Str[i+1:i+4] != ' B(' \
            and wf_change_Str[i + 1:i + 7] != ' and B':
        indexA = i
    if wf_change_Str[i] == ' '  and wf_change_Str[indexA] == 'A' \
            and wf_change_Str[i+1:i+4] != '127' \
            and wf_change_Str[i + 1:i + 6] != 'ctive'\
            and wf_change_Str[i + 1:i + 4] != ' B(' \
            and wf_change_Str[i + 1:i + 7] != ' and B':
        test_str = wf_change_Str[indexA+1:i]
        test_float=float(test_str)
        new_c_str = new_c_str + 'A' + str(valueA)
        valueA = test_float * incrementA
        valueA = round(valueA, 5)
        indexA = i
    # --------------- ends in comma --------------------
    if wf_change_Str[i] == ';'  and wf_change_Str[indexA] == 'A' :
        #print('enter', 4)
        test_str = wf_change_Str[indexA+1:i]
        test_float=float(test_str)

        valueA = test_float *incrementA
        valueA = round(valueA, 5)
        new_c_str = new_c_str + 'A' + str(valueA) + ';'
        indexA = i
    elif wf_change_Str[indexA] != 'A':
        new_c_str = new_c_str + wf_change_Str[i]
    i = i + 1
```

Figure 6 - G-code Parser, multiplier application

```
i = 0
list = []
startIndex = 0
ifEnter = 0
while i < len(new_c_str):
    if(new_c_str[i-1] == 'T' and new_c_str[i] == '1'):
        list.append(new_c_str[startIndex:i+1])
        startIndex = i+1
        ifEnter = ifEnter + 1
    i = i+1
#if this print is only one extruder
if ifEnter == 0:
    list.append(new_c_str)
# ------------------------------------------------------------------
# insert list into wf_same_Str at * positions
i = 0 # same_string position
j = 0 # list position
while j != len(list):
    if wf_same_Str[i] == '*':
        wf_same_Str = wf_same_Str.replace(wf_same_Str[i],list[j],1)
        j = j + 1
    i = i + 1
i = 0
# ---------------- Right Prime Hotfix -------------------
#rep = wf_same_Str.find('A0.65725')
#wf_same_Str = wf_same_Str[0:rep] + 'A25.000' + wf_same_Str[rep+8:]
# ------------------------------------------------------------------------
x = wf_same_Str.find('; End of print')
final_Str = wf_same_Str[0:x] + end
# ------------------------------------------------------------------
# write to finish file
file_fin = file + '-fin-'+ str(incrementA) +'.gcode'
with open(file_fin, 'w') as wff:
    wff.write(final_Str)
print('Done! ' + file_fin + ' file created!')
```

Figure 7 - G-code Parser, final assembly

Figure 6 displays the part of the program that applies to multiplier to the linear actuator section of the G-code. Figure 7 assembles the new lines of code into a new G-code file that is now ready for bioprinting. The assembly appends the text, “-fin-” and the multiplier value to the end of the filename denoting the finished version of the G-code and the multiplier value.

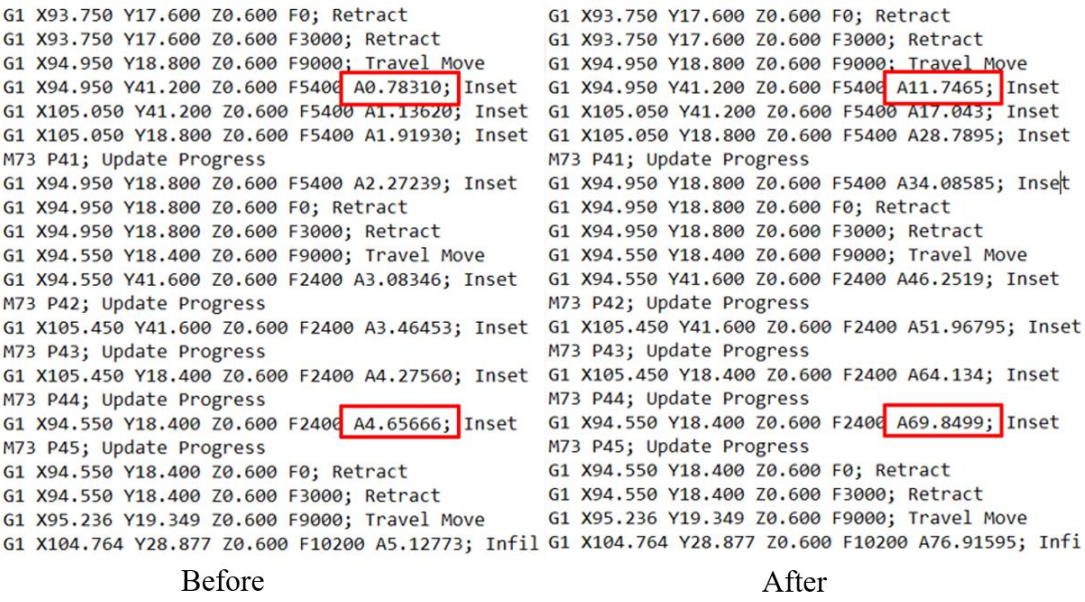

Figure 8 - G-code example, before and after

An example of the before and after of using this parsing program is displayed in Figure 8. On the left is an example of G-code before running through the parsing program, and on the right is the G-code after. The changes in code can be seen within the red boxes of the before and after images. A multiplier of 15 was applied and the results in the right image show a successful conversion of the G-code.

2.2.4. Flow Chart of Print Process

The process for printing is not straightforward. There are multiple steps that must be performed in order to prepare a G-code file for bioprinting. These steps can be visualized in Figure 9. The first step is to export a CAD file as an STL file. Next the user opens the STL file in MakerBot Desktop and slices the STL file into G-code. This G-code is then converted for bioprinting via the parsing program. The MakerBot printer used for this project only uses x3g file types. As a result, a conversion program, GpxUI

obtained from https://www.thingiverse.com/thing:81425/comments, was used to convert the G-code from x3g to GpxUI. After the x3g file is obtained, the file is ready to be bioprinted.

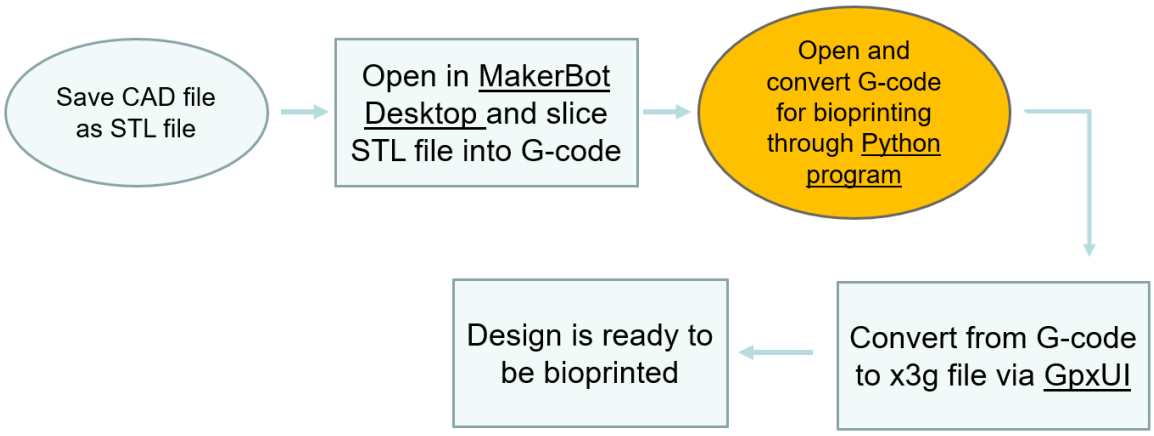

Figure 9 - Bioprinting Flow Chart

2.2.5. Preparation and analysis of hydrogel solution

The hydrogel solution used in this study mainly consist of PEGDA and PAA. PEGDA with molecular weight 1000 Da was purchased from Monomer-Polymer and Dajac Labs. The following chemicals were purchased from Sigma Aldrich, Polyethylene oxide (PEO), Acrylic acid (AA) monomer (anhydrous), 2,2-Dimethoxy-2-phenylacetophenone, and 1-Vinyl-2-pyrrolidinone. The photo-initiator solution was prepared by mixing 2,2-Dimethoxy-2 phenyl acetophenone in 1-Vinyl-2-pyrrolidinone [15]. A drop of orange food coloring dye was added to give the solution a non-transparent color.

2.2.6. Polycaprolactone Filament Molecular Weight Analysis

The PCL filament used for this study was 3D TWP 1.75mm PCL material filament which was purchased from Amazon. To analyze the properties of this material, an Agilent 1200 series HPLC/SEC System was used to perform gel permeation chromatography and size exclusion chromatography (GPC/SEC). The flow rate used was 1 mL/min. DMF was used as a solvent.

2.2.7. Hydrogel Viscosity Analysis

Characterizing the viscosity behavior of our hydrogel was important for defining the capabilities of our bioprinter. A Kinexus Ultra cone and plate rheometer was used for this study. The cone had an angle of 4° and a diameter of 40 mm. The temperature of the rheometer was set at 25°C. The gap size was 0.15 mm. The shear rate was ramped from 0.1 to 10 s-1 over 5 minutes.

2.2.8. Printer Efficacy Analysis

High accuracy and precision are key characteristics to additive manufacturing. Therefore, it was necessary to analyze our 3D bioprinter print quality. To test the limits of the bioprinter's resolution, we used ImageJ to analyze printed lines of thermoplastic and hydrogel respectively. Analysis was done by quantifying the width of printed lines at various intervals along the construct. ImageJ software was used to quantify the widths. Each group had a sample size of four.

2.2.9. Mechanical Testing

Scaffolds were printed at 12.7 mm x 25 mm for mechanical testing (n=5). All samples, unless specified, were soaked in PBS for one hour prior to being place in an Instron 5869 mechanical testing machine. The gauge length for each sample was measured prior to being strained at 5 mm/min until failure or plateauing. The elastic modulus, yield strength, and ultimate strength were calculated from each sample. The elastic modulus, yield strength, and ultimate strength are reported as an average with standard deviation. All mechanically tested products were printed with the 20-gauge tips.

2.3. Results

2.2.1. Dual Head 3D Bioprinter Fabrication

To make bioprinters more readily available, we have created a 3D printable microextrusion device that can be outfitted to an open-source thermoplastic-based 3D printer. By setting one of the two OEM stepper motors into the vertical position, the motor can drive the microextrusion device. The setup of the printer is shown in Figure 10. The microextrusion device in highlighted by the red circle. On the right side of the printer is the ultraviolet light lamp used for cross linking. On the front of the printer is a protective shield to keep users safe from the UV light. All other open portions of the printer are covered to prevent UV light from escaping the print area. Also included, but not shown, is a hood that sits on top of the printer that offers additional protection to users.

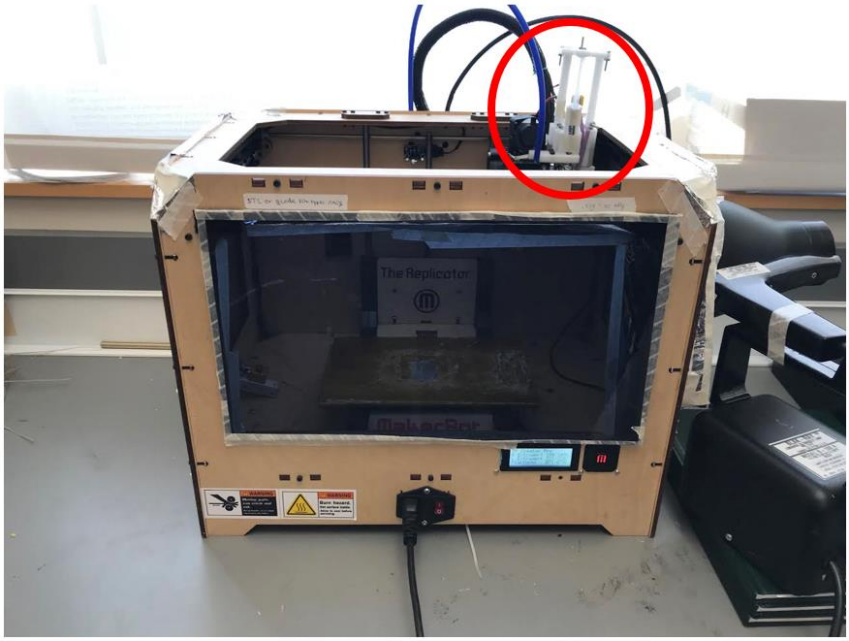

Figure 10 - Full setup of MakerBot Biprinter

2.2.10. Bioprinter Resolution and Accuracy

To examine the accuracy of our printer, we quantified the width of printed bioink and thermoplastic lines using ImageJ software to define positional accuracy. The needles used in this study were 18, 19, 20, 21, and 22 gauge. A PCL thermoplastic print line was used as a control and point of comparison. The thermoplastic print head had an inner radius of 0.4 mm. Ideally, we want our bioink prints to have a width equal to the thermoplastic control print line.

The 18-gauge syringe tip yielded the worst print line with an average width of 3.18 mm. This is significantly larger than the 19-gauge syringe tip which had an average width of 1.47 mm. There was no significant difference between the average widths of the 19, 20, 21, 22, and PCL control. However, the PCL control yielded the smallest average width of 0.89 mm. The 22-gauge tip yielded the closest average width of to the PCL

control. Overall, bioprinting efficacy improved by reducing the size of the tip. Differences in thermoplastic and hydrogel prints decreased significantly ($p \leq 0.05$) as the size of the tip was reduced.

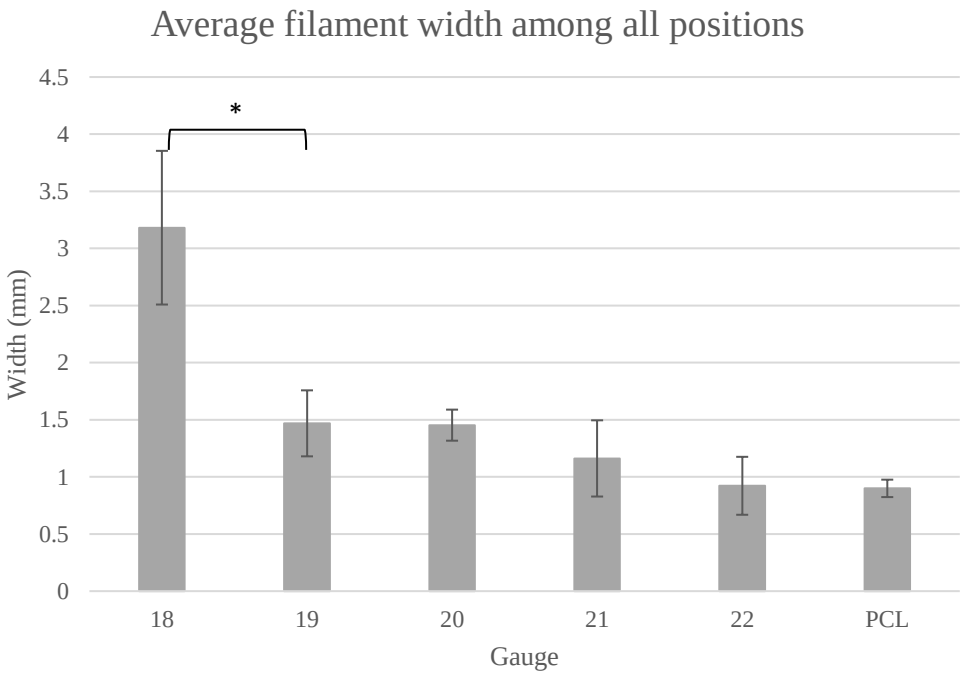

Table 1 - Printer efficacy summary (n=4)

2.2.11. Bioprinted Scaffolds

Shown below in Figure 11 are complex scaffolds fabricated by our bioprinting system. It should be noted that the process for printing these scaffolds is completely automated. Listed in row A is our first printed scaffold which we refer to as a sandwich. The red solids represent two individual layers of PCL. The gray solid represents a layer of our hydrogel solution. During the print process our system deposits a layer of PCL, switches to and deposits a layer of hydrogel. After the hydrogel layer is extruded the printer homes all axes and pauses for seven minutes in order to let the hydrogel crosslink

via the UV light. The printer then switches back and lays down a layer of PCL. The final product is shown in the right-most image in row A. Row B displays a PCL imbedded hydrogel. PCL fibers are printed between two layers of hydrogel. The first layer of hydrogel is deposited and crosslinked for seven minutes and PCL fibers are deposited on top. The second layer of hydrogel is then deposited and crosslinked for another seven minutes. In row C is a PCL box with hydrogel crosslinked inside. First a PCL box is printed, and hydrogel is deposited inside. Again, the hydrogel is crosslinked for seven minutes. A final layer of PCL is then deposited on top.

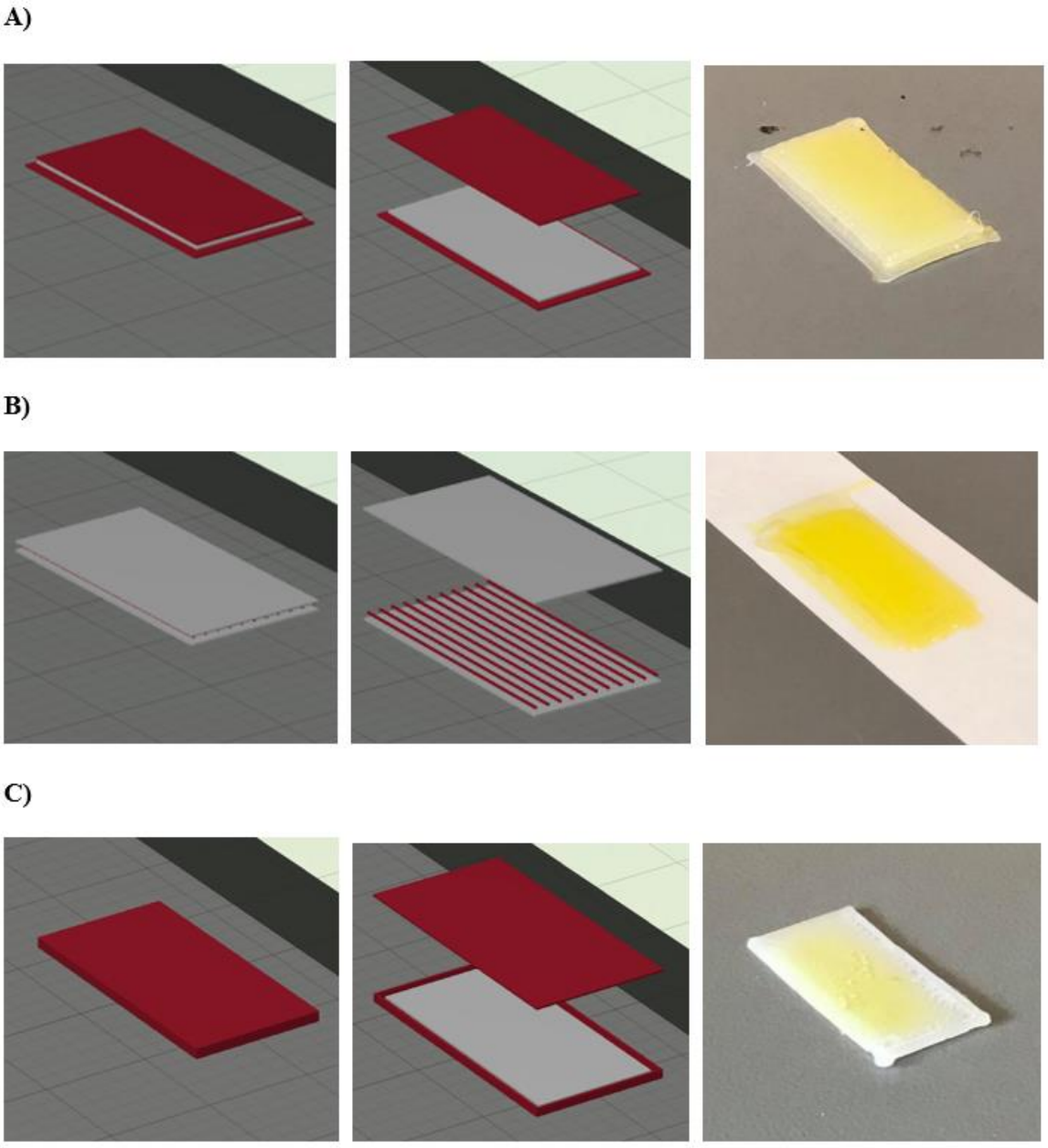

Figure 11 CAD rendering and final product images of complex bioprinted hydrogel scaffolds. CAD renderings are shown on in the first two columns from the left. The final real-world print is shown on the right. A) Hydrogel sample sandwiched between two layers of PCL, B) Hydrogel sample housed inside a PCL box, and C) PCL fibers sandwiched between two layers of hydrogel.

2.2.12. PCL Filament Molecular Weight

GPC/SEC analysis of our PCL filament yielded a molecular weight of 41 kDa and molecular number of 32 kDa. The polydispersity index was determined to be 1.3.

2.2.13. Hydrogel Viscosity

By ramping our shear rate from 0.1 to 10 s-1, our viscosity appears to have a nonlinear shear thickening behavior. The hydrogel was stored in at a refrigerator at 4°C. During testing the material was not refrigerated, therefore the material would get warmer throughout testing. This could attribute to the variation in hydrogel viscosity. However, generally the viscosity rose as shear rate increased.

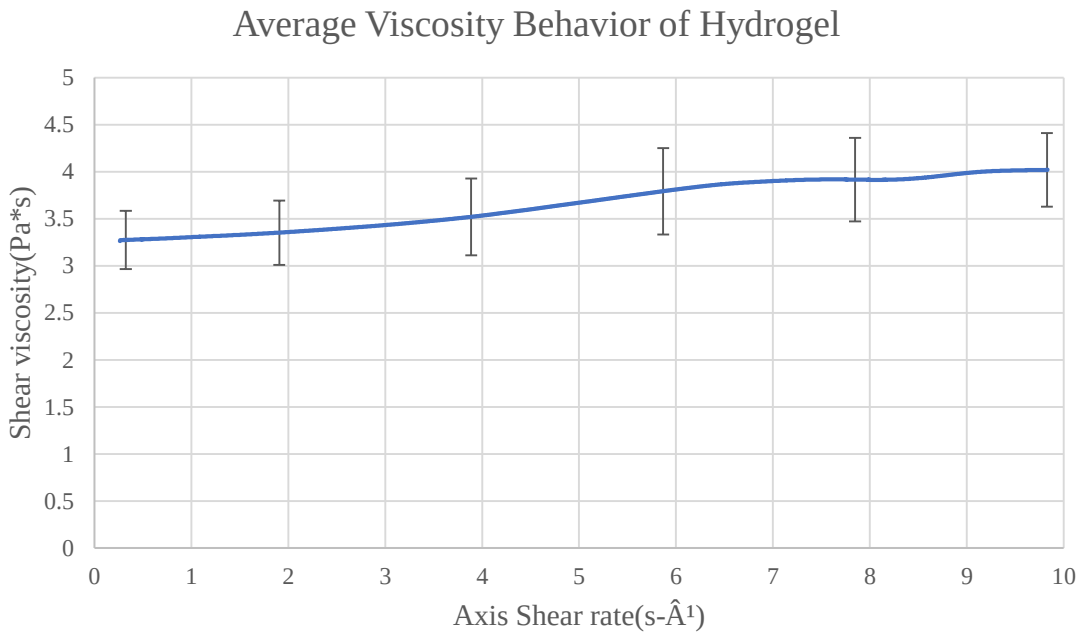

2.2.14. Mechanical Testing of Printed Scaffolds

Prior to mechanical testing all samples were soaked in PBS for 60 minutes unless otherwise stated. The samples used in this study include a hydrogel, PCL, one layer of

PCL and one layer of hydrogel (PCL-hydrogel), hydrogel with imbedded PCL fibers (PCL-hydrogel-imbed), PCL-hydrogel sandwich, and PCL-hydrogel-box. We first determined the young's modulus of our samples. After analysis, it was necessary to separate samples made mostly of hydrogel from samples made mostly of PCL as the hydrogel samples displayed significantly lower mechanical properties. The young's modulus of the hydrogel with imbedded PCL fibers had significantly higher young's modulus than the hydrogel scaffolds (Figure 12). The young's modulus of the PCL-hydrogel sandwich was significantly greater than all other samples shown in Figure 13 except the PCL soaked sample. The soaked box sample had significantly higher young's moduli than the non-soaked box samples.

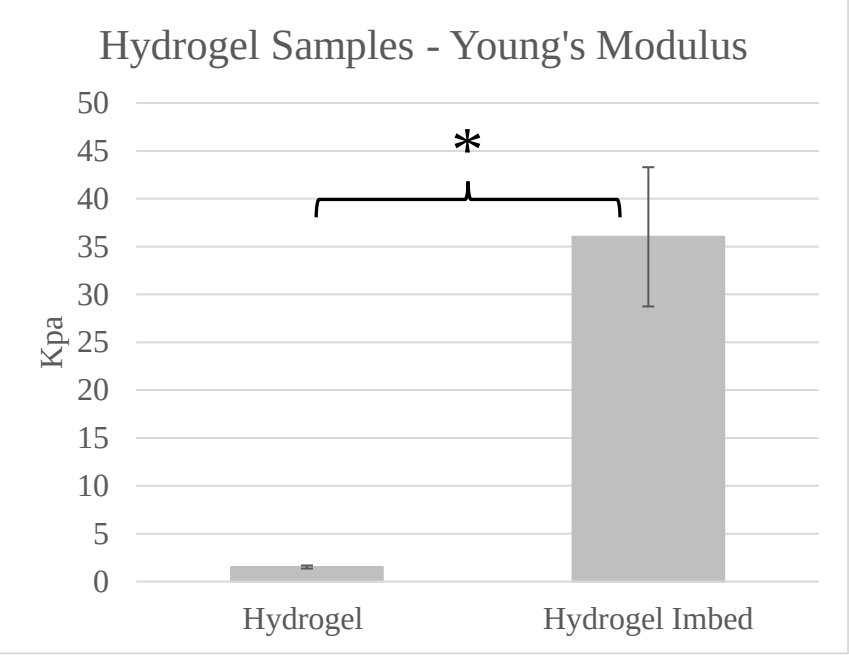

Figure 12 - Young's Modulus of Hydrogel samples

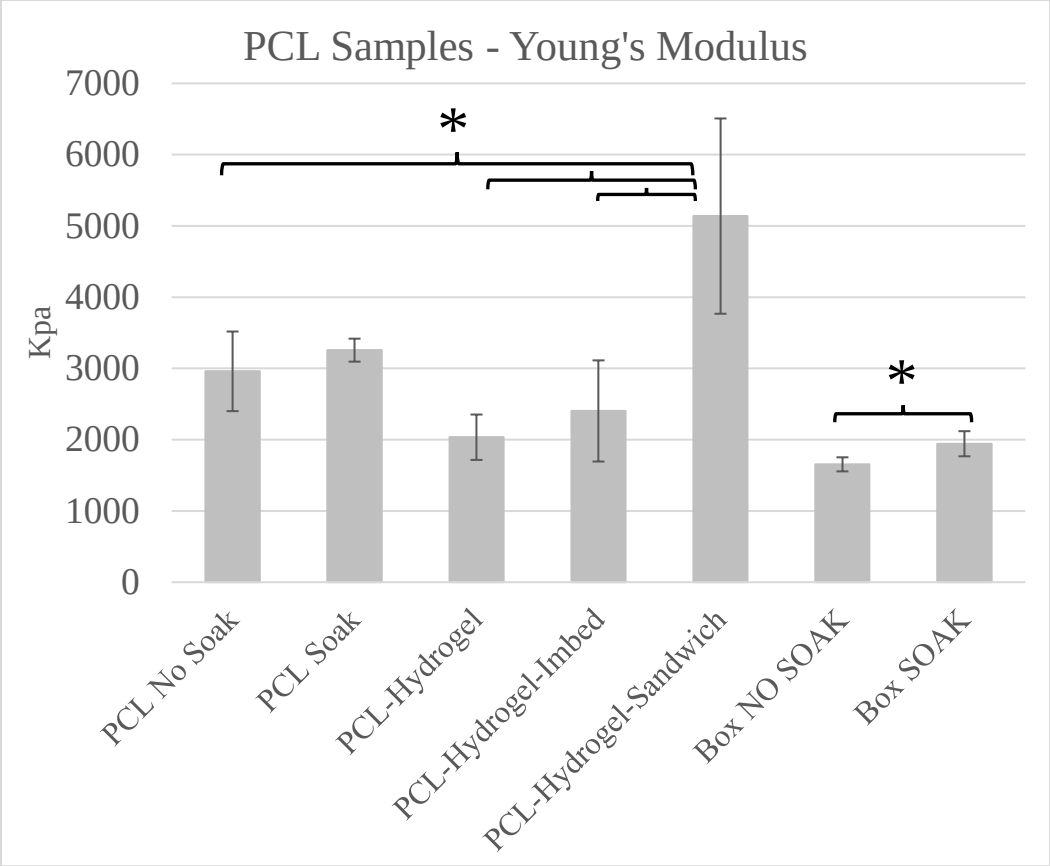

Figure 13 - Young's Modulus of PCL samples

The yield strength for the samples made mostly of hydrogel was not recorded as these samples failed at their ultimate strengths. There was no significant difference in ultimate strength between the hydrogel sample and hydrogel samples imbedded with PCL fibers (Figure 14). For samples constructed mostly from PCL, the PCL-hydrogel-sandwich displayed significantly higher yield and ultimate strengths than PCL-hydrogel and PCL-hydrogel-imbedded samples. There were no significant differences between soaked and non-soaked PCL samples. There was a significant difference in yield and ultimate strengths between soaked box and non-soaked box scaffolds (Figure 15).

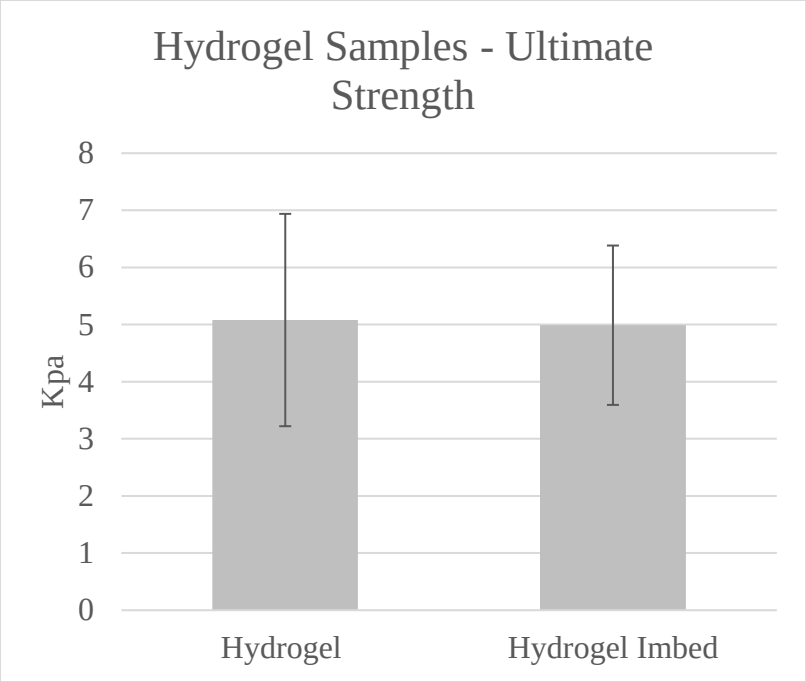

Figure 14 - Ultimate Strength of Hydrogel samples

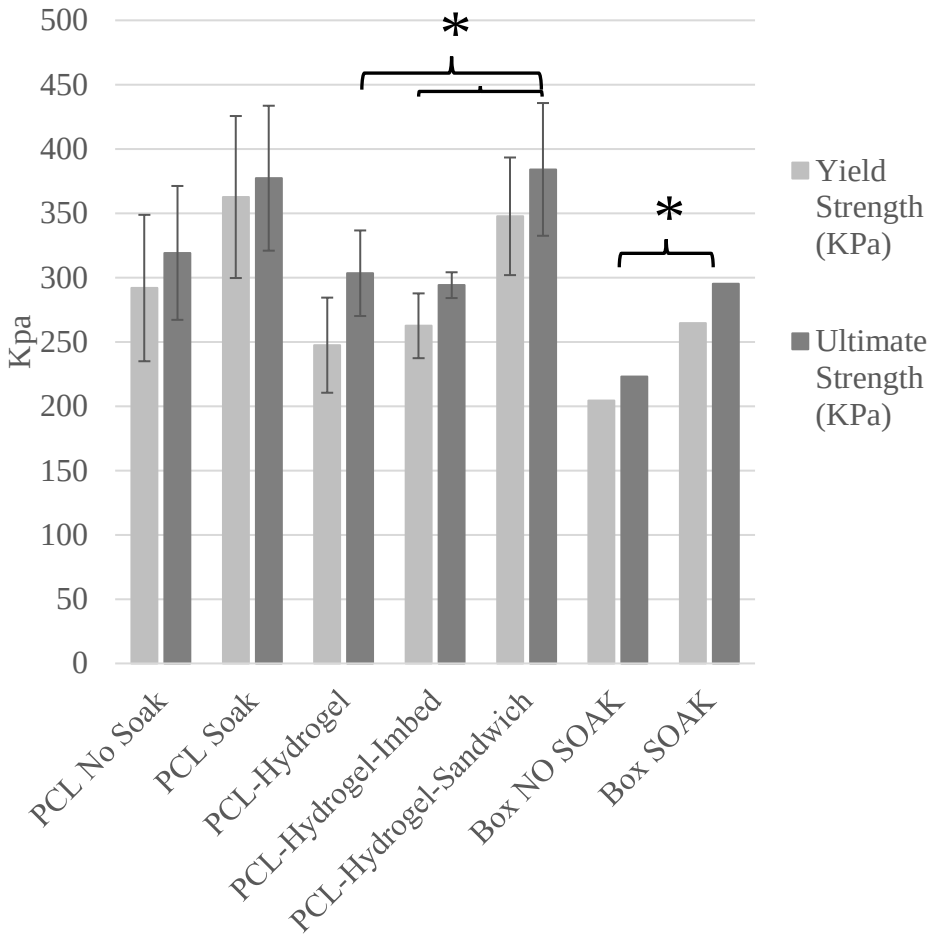

Figure 15 - Ultimate Strength and Yield Strength of PCL samples

2.4. Discussion

By using a commercially available 3D printer and a 3D printed microextrusion device, we are able to reliably and precisely deposit bioinks and thermoplastics to fabricate complex scaffold constructs. Similar to the bioprinting system developed by Hinton et al. [22], our technique implements the use of a modified MakerBot Replicator modified with a custom screw driven syringe extruder for bioink deposition. However,

unlike Hinton et al., we are able to print bioinks without the need of a secondary support bath. Our bioprinting system can deposit bioink materials at a similar print width to that of thermoplastic materials. This accuracy can be attributed to the use of 19+ gauge size needle tips and the high precision movements of stepper motors.

Compared to other pneumatic based bioprinting systems, our system has shown a comparable ability to print consistently accurate structures. The main concern of this study was to reduce the width of bioprint lines to the point where they were equal to the width of thermoplastic print lines. Other studies were concerned with the print height for each layer [17]. Our system was able to achieve a print width very close to that of a thermoplastic print. The system however could not print thinner than the thermoplastic print. The limiting factor of this was the gauge size of the needle and hydrogel viscosity. Due to the high viscosity, we were unable to deposit inks through gauge sizes higher than 22. If the viscosity of the material was lowered, we could theoretically extrude thinner print lines. However, we decided to maintain this high viscosity so that after the material is deposited, it would not disperse and lose its shape. The need for high viscosity bioinks could also be corrected if the cross-linking time of our material was instantaneous. A higher viscosity was needed to maintain the structural integrity of print lines as cross linking was not instantaneous. The lines were required to maintain their shape for seven minutes before being cross-linked. If cross linking times were reduced to instantaneous, the need for higher viscosities solutions would not be a necessity.

A disadvantage the screw-based extrusion method is the inability to start and stop depositing liquid instantaneously. This is due to the driving plate of the linear actuator still moving after the stepper motor has been commanded to stop. Future work should

aim to incorporate a pneumatic pressure-based extrusion method in order to solve this issue.

In previous studies, it has been shown that the length of the dispensing nozzle has negative effects on human pluripotent stem cell viability [23]. Studies have demonstrated that cells printed through an 8.9 mm nozzle length displayed higher levels of cell viability that those printed through a 24.4 mm nozzle length [23]. The nozzle lengths used in our study were 38.1 mm which are significantly longer than that used by Faulkner-Jones et al. This nozzle length was necessary in order to reduce the amount of modifications made on original MakerBot Replicator. Future iterations should make use of a shorter dispensing nozzle length to ensure a higher level of cell viability. Additionally, screw based microextrusion techniques can potentially generate a pressure drop along the nozzle resulting in harmful stresses being inflicted on loaded cells [16].

Mechanical testing of the young's modulus and ultimate strength yielded results that were significantly lower than that of hydrogel samples seen in Browe et al. [15]. The reason for these lowered mechanical properties can possibly be attributed to air bubbles forming in the hydrogel during the printing process.

In addition to the printer's functionality, it is also significantly cheaper compared to commercial bioprinters currently on the market, costing less than $200. By analyzing the market and looking at the lower end of the cost range, one company provides one, two, three, and six head extruding bioprinters which range in cost from $8,750 up to $50,000. Another company two and three head extruding bioprinters at prices of $11,840 and $29,140 [17]. Although these bioprinters offer more versatility and functionality than our system, the cost ranges from 43X to 250X the price required to build our bioprinting

system. Thus, our 3D bioprinting system offers a functional and cheaper alternative to commercially available systems.

The low-cost of this bioprinter was achieved by mostly using mechanical parts that came with the printer. The stepper motor used to drive the bioink depositing linear actuator was included with the printer. We also designed our 3D printed linear actuator around the current layout of the print carriage, which reduced the need to buy additional components. Additionally, designing the linear actuator to be 3D printed significantly reduced the cost of our printer. The only components that were purchased include flexible couplings which was used to connect the linear actuator screw to the stepper motor, syringes, and syringe tips. However, although the material costs were low, a significant amount of intellectual capital was necessary to make the necessary code changes. These changes and the python code used to make them could be applied to other systems, reducing the amount of new coding necessary to start printing.

2.5. Conclusion

By using 3D printed components and Python coding, we have developed a low-cost screw-microextrusion-based bioprinter that introduces an interesting alternative to commercially available bioprinters. We designed a 3D printable linear actuator modification and a parsing program that converts a low-cost 3D printer into a functional 3D bioprinter. This bioprinter can construct complex tissue scaffolds with a high level of print accuracy. We characterized this print accuracy along with the mechanical properties of fabricated tissue scaffolds. Future work will focus on creating different hydrogel formulations of various viscosities and test them using different print heads to achieve new levels of print accuracy. Furthermore, printing cells using this system and testing

their viability in constructed prints will be key to determine this bioprinters application with fabricating cell-laden tissue scaffolds. The addition of pneumatic pressure driven deposition could also provide additional control and precision when printing.

CHAPTER 3: THE DEVELOPMENT OF A LOW-COST TRIPLE HEAD PNEUMATIC PRESSURE DRIVEN 3D BIOPRINTER

3.1. Introduction

In this study we hypothesize that based on our preliminary projects, a low-cost triple head 3D bioprinting system can be achieved by fabricating parts out of 3D printable materials and implementing a custom pneumatic pressure system as a deposition method. Our objective was to develop a pneumatic pressure-based system that is capable of depositing thermoplastic and bioink materials. We will further improve upon the design of our previous 3D bioprinting system that was constructed in a preceding study. Most of the components used to build this new system will be 3D printable in order to lower the cost of construction. The pneumatic pressure system will function using three solenoid valves and an Arduino microcontroller which will allow for the accurate dispensing of multiple biomaterials. Custom software will be designed in order to allow the bioprinting system to function properly.

3.2. Materials and Methods

In this section, we define the components and individual methods of the printer and then summarize how each contributes to the full system. The main components of the bioprinting system include the base 3D printer, printer modifications, and the Ardunio

circuit that controls three solenoid valves. In our design we use the 3D printer to send signals to the Arduino and control the state of the three solenoids. This control system is necessary to achieve pressure driven bioprinting.

3.2.1. Base 3D Printer

In order to simplify the build process for this 3D bioprinter, we decided to build of an existing DIY 3D printer kit. The printer used was a HE3D EI3 3D Triple Extruder Printer. The x, y, and z axes were the main components used from the kit. All other components used for creating the 3D bioprinting system were purchased or 3D printed. It should be noted that the original 3D printer is designed to be a triple extruding system that can deposit three thermoplastics within a single print. In addition, this printer runs off Reprap Prusa i3, an Arduino based 3D printing firmware.

3.2.2. Modifications to the 3D printer

Two modifications were purchased for the 3D printer. The first modification was a new MOSEFT (metal-oxide semiconductor field-effect transistor) that can handle the high-power heating requirements of the print bed. The original MOSFET did not have a heatsink which caused the it to become dangerous when heating the print bed. The new MOSFET is capable of withstanding large amounts of power making it more convenient for machine use while also reducing the danger associated with serious heating. The new MOSFET used was a BIQU Heat Bed Power Module Expansion which is shown on the right of Figure 16.

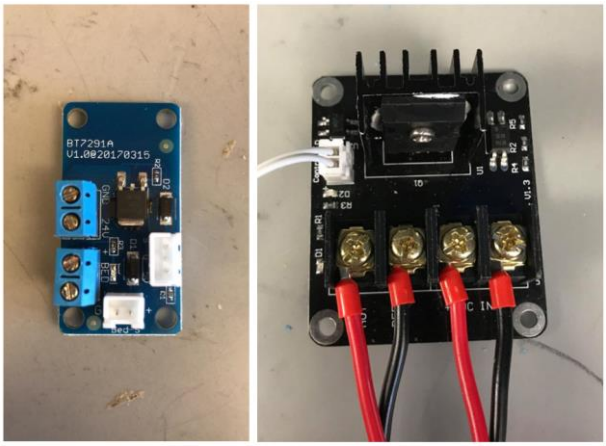

Figure 16 MOSFET Replacement, left: original MOSFET, right: new MOSFET

The second purchased modification was a single head thermoplastic extruder. This was a necessary addition in order to remove the bulky heatsink that was paired with the original triple head extruder that came with the printer. This also allowed for design flexibility when planning the addition of syringes in place of the two other extruders. The extruder used was a Wangdd22 3D Printer J-head Hotend, 1.75mm, 12 Volt Extruder.

The following modifications were 3D printed in order to fulfill project specific needs. A new carriage was designed in order to incorporate the new J-head extruder along with two syringes. The carriage was designed into the following three separate components: base, z-sensor attachment, and syringe mount. The base, Figure 17, is designed to be very similar to the original carriage with a few minor modifications, the most notable being the incorporation of the J-head extruder seen on the left side of the base. Two mounting points were added to allow for easy removal of the J-head extruder. Additional holes were cut for mounting other components.

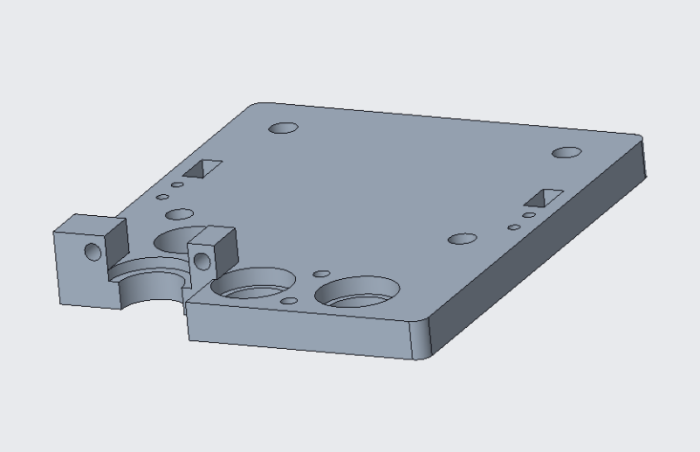

Figure 17- Carriage Base

The z-sensor attachment, Figure 18, serves as both an attachment point for the z axis sensor and an enclosure for the J-head extruder. The attachment point is designed like a rail in order to allow the z-sensor to be adjusted easily. The enclosure allows for easy removal and installation of the J-head extruder by use of two screws that connect with the base.

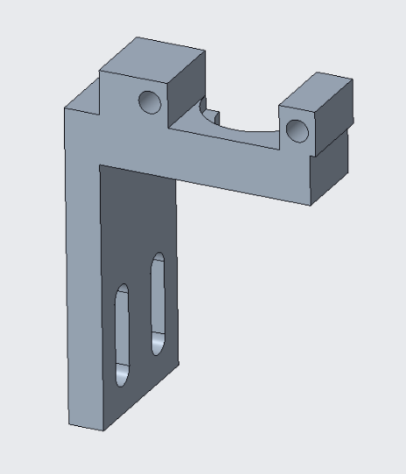

Figure 18 - Z-Sensor Attachment

The last 3D printed component was the syringe mount, Figure 19. This mount is designed to house two 5 mL syringes. Two holes located at the base of the mount are

used with screws to secure the syringes into place so that they do not move during the print process.

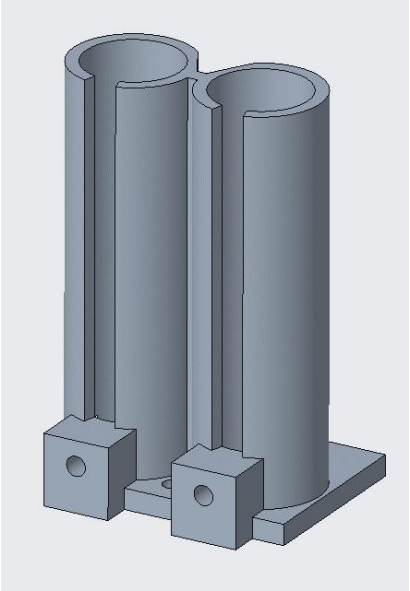

Figure 19 - Syringe Mount

Another 3D printed component is the syringe-tubing connector shown in Figure 20. This connector links the pneumatic pressure tubing and the syringe together which allows air pressure to drive the fluid within the syringe. The assembled carriage is displayed in Figure 21. The two syringes and thermoplastic extruder are also installed.

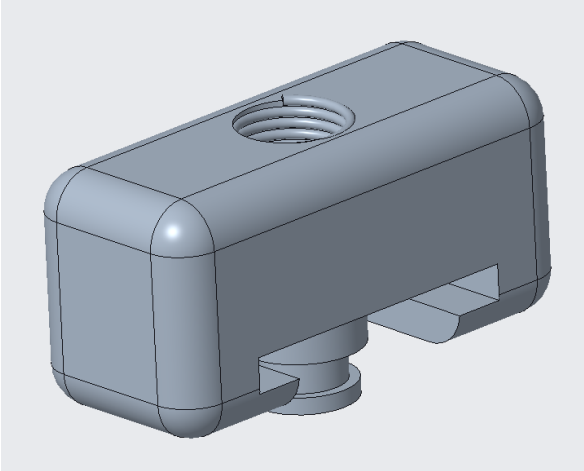

Figure 20 - Syringe-Tubing Connector

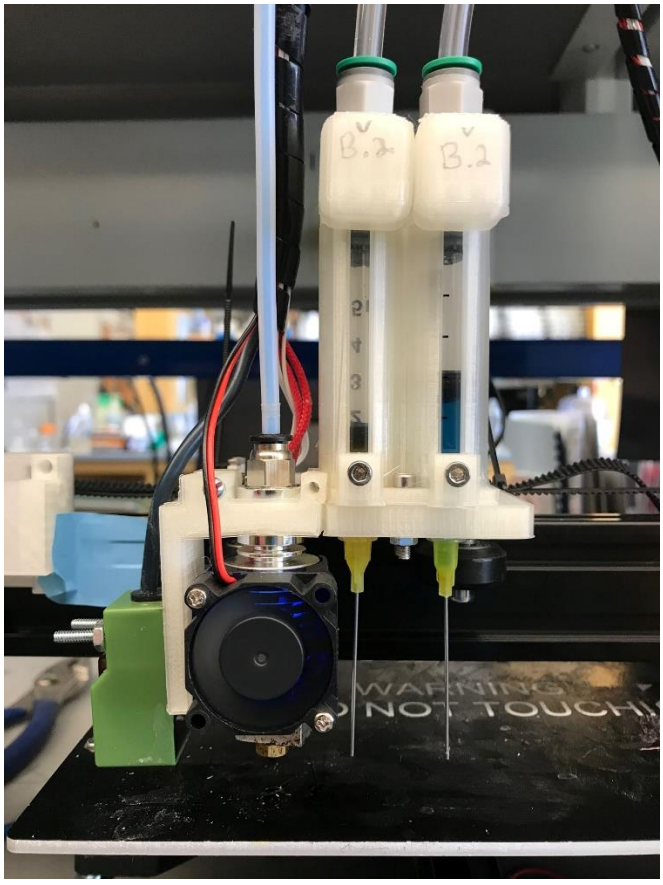

Figure 21 - Assembled Carriage with Thermoplastic Extruder and Syringes

Other 3D printed components used in this project included a solenoid-tubing connector and a 3-way air splitter. The solenoid-tubing connector was downloaded from: https://grabcad.com/library/barb-fitting-1. The air splitter was downloaded from: https://www.thingiverse.com/thing:401163. Downloading these components saved time during the development of the printer.

3.2.3. 3D Printer Firmware

In order to digitally connect the Arduino system to the 3D printer, edits to the printer firmware were made. Arduino based 3D printing firmware is organized into the following types of files: CPP file, H file, BAK file, and Arduino file. The first edit was done in file HAL.cpp and is only required for users working with Arduino versions 1.6.10 or later. Without the following edit, the user will encounter a compiling error and will be unable to upload the firmware to the 3D Printer. The edit occurs in line 666 of HAL.cpp and requires users to replace the phrase "long stepperWait = 0;" with "long __attribute__((used)) stepperWait = 0;". This edit allows users to upload this firmware to the 3D Printer.

The next edit occurs in the file pins.h. In order to connect the 3D printer to the Arduino microcontroller, unused digital pins on the 3D printer were used. Of the two available digital pins on the 3D printer, pin 12 was define as a "sensitive pin." This definition prevents users from being able to set pin 12 to a specific value resulting in the inability to send signals from the 3D printer to the Arduino using that pin. In order to overcome this problem, the phrase "ORIG_PS_ON_PIN" must be removed from line 2864 of pins.h. This removal will allow users to send signals to pin 12 of the 3D printer's motherboard.

3.2.4. Repetier-Host setup for printing

The program used to control the 3D printer when it is connected to a computer is Repetier-Host V1.5.4. Various changes to the slicing settings were required in order to make this printer suitable for bioprinting. In order to change the settings, a custom .ini file was created. Only the thermoplastic extruding print head of the printer needs to be heated during printing. In the .ini file extruder 1 was set to 250°C, extruder 2 was set to 0°C, and extruder 3 was set to 0°C. The print bed was set to 60°C. These settings assume PLA is being used as a thermoplastic. Additionally, within the print settings of Slic3r, all rafts were turned off and the overhand threshold was changed to 90.

3.2.5. Pneumatic Pressure System and Solenoids

Three direct acting solenoids manufactured by Yosoo were used to create this bioprinter, Figure 22. These solenoids are 2 way and are normally closed in a deenergized state. Applying a 12-volt current to the solenoid causes the valve to be energized and open, allowing air to pass through. Using direct acting solenoids was more suitable for creating this bioprinter as they do not require external pressure along with electrical current to open, the electrical current was provided by the Arduino microcontroller and an external power supply. Displayed in Figure 23 is the flow setup of the three solenoids. The air source is connected to the three solenoids by 1/4” tubing and the 3-way air splitter. A relief solenoid was designed into the system to prevent any backpressure from building up which could cause damage to the tubing and solenoids.

Figure 22 - Solenoid Valve

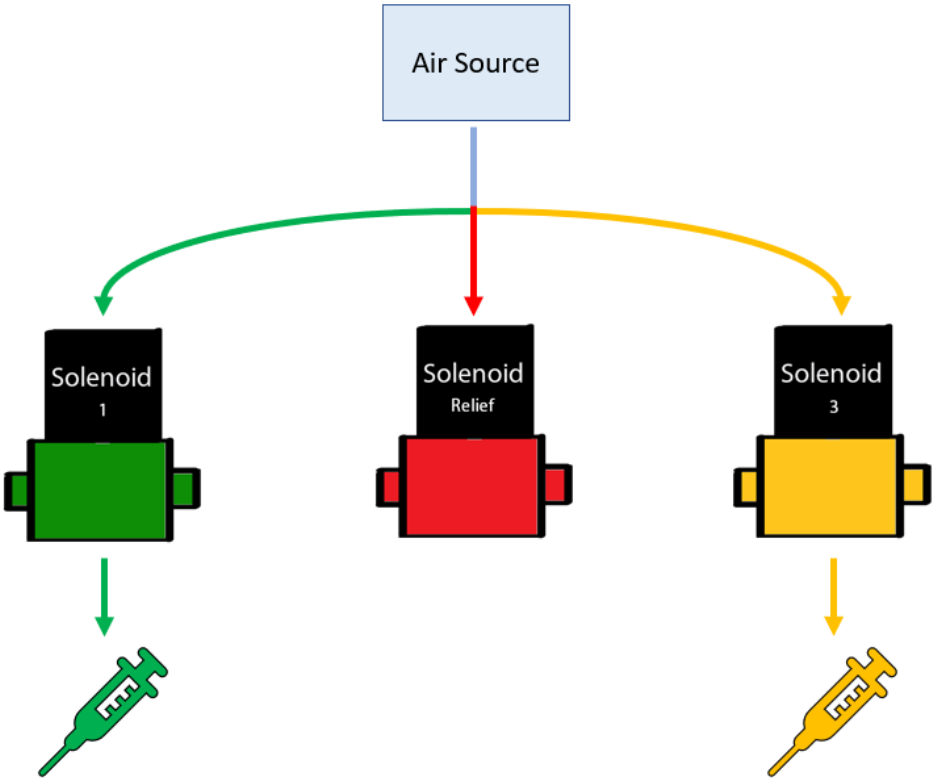

Figure 23 - Solenoid Flow Setup

3.2.6. Arduino to Printer Communication Circuit

Establishing communication between the 3D printer and solenoids was a major part of this project. It was imperative that the printer could digitally control all three solenoids from corresponding G-code files. This was achieved by introducing an Arduino microcontroller which would receive signals from the printer, interpret them, and subsequently command the solenoids to perform specific actions. Pins 11 and 12 on the 3D printer were connected to the Arduino and served as the main communication link between the two systems.

In order to control the output of signals from printer, the following line of G-code was used, “M42 Pnnn Snnn”. M42 is a command used in G-code to trigger a general purpose I/O pin [24]. Pnnn represents the pin number while Snnn represents the pin value. Pin values can range from 0 to 255, where 0 is considered off and 255 is considered on. We use I/O pins 11 and 12 on the printer as our output signal pins which will be sent to the Arduino for interpretation. By using the M42 command, we can set these pins to either 0 or 255. Initially only D11 was available for use as a general purpose I/O pin. However, thanks to the firmware edits made in section 3.2.3, it became possible to use pin D12 as an I/O pin.

Pins D11 and D12 on the printer connect to the Arduino at pin 2 and pin 3. These Arduino pins would receive the signal, 0 is considered off, and 255 is considered on. By using the versatility of the Arduino microcontroller, three LED’s and two limit switches were wired together in addition to the three solenoids. The three solenoids are controlled by TIP120 transistors. The LED’s were used to indicate which solenoids were on and off. The two limit switches were used as a troubleshooting tool. When triggered, the limit

switches would manually turn on and off the corresponding solenoids. A full schematic of this circuit is shown in Figure 24. The design for this circuit is based off the schematic made publicly available on https://www.bc-robotics.com/tutorials/controlling-a-solenoid-valve-with-arduino/. Refer to section 3.2.7 for in-depth explanation on the Arduino coding used.

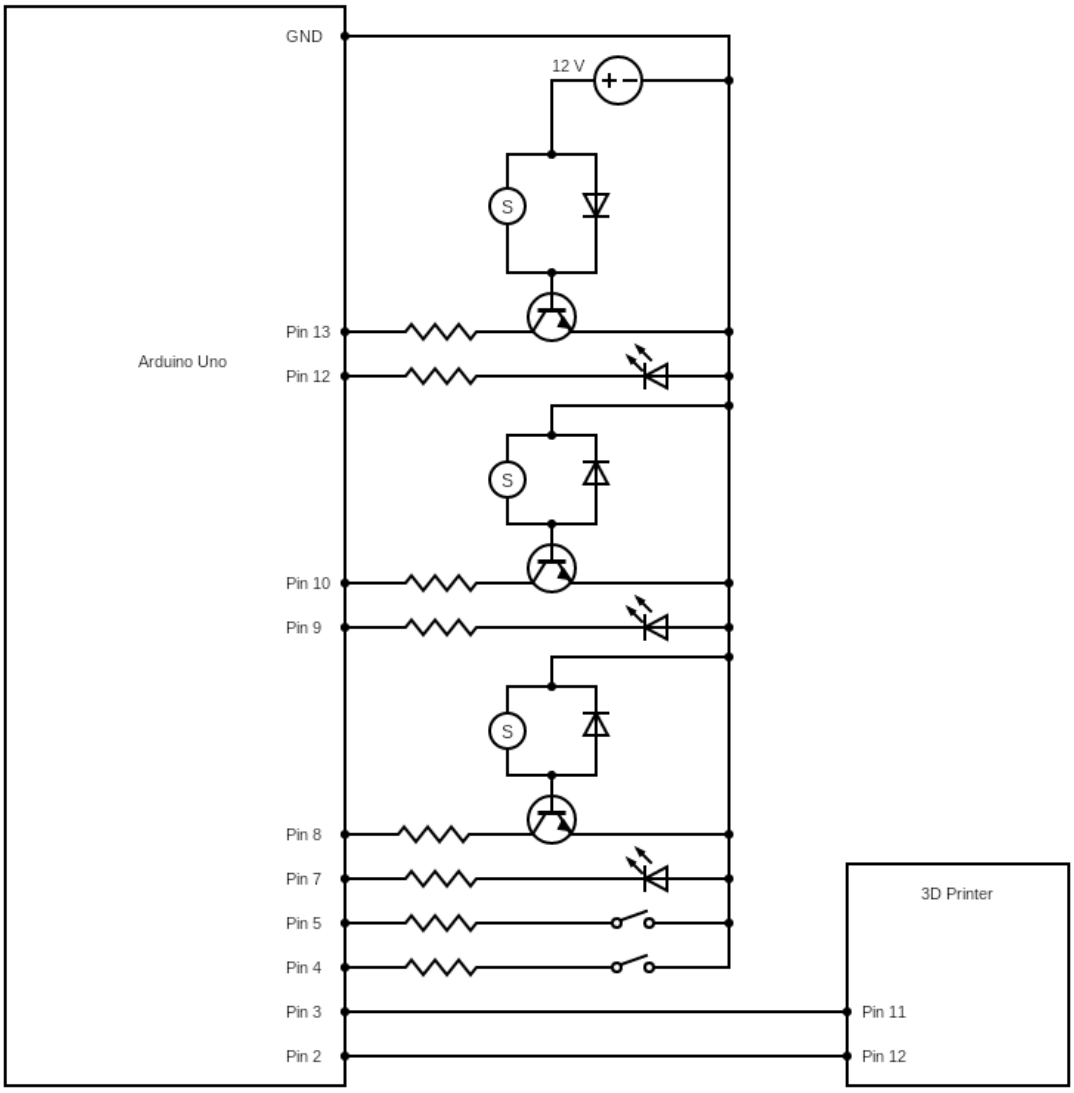

Figure 24 - Arduino/Printer Communication Circuit

3.2.7. Arduino coding

The Arduino is the link between the printer and the solenoids. The coding of the Arduino interprets the printer signals from D11 and D12 and decides which solenoids need to be on and off. Shown in Figure 25 and Figure 26 is the code used to create this bioprinter. In Figure 25, relevant variables and initial conditions are defined. Both solenoid 1 and 3 and their respective LED's are initially off while the relief solenoid and it's LED is on. It can be assumed that when stating a specific solenoid, the corresponding LED state is associated with it.

Shown in Figure 26 is the valve control loop which defines when the solenoid should be open or closed. Within the loop, if the Arduino reads a value of 255 from D11, solenoid 1 will open while the relief solenoid and solenoid 3 close. A similar action occurs when a signal is received from D12 however solenoid 1 is closed while solenoid 3 is opened. Although the printer can output a signal from 0 to 255, the Arduino interprets the signal is either 0 or 1. A value of 1 will only be achieved when the Arduino receives a signal of value 255.

```
int solenoidPin1 = 13;
int led1 = 12;
int solenoidPin2 = 10;
int led2 = 9;
int solenoidPin3 = 8;
int led3 = 7;
int switch1 = 2;
int switch1State = 0;
int switch2 = 3;
int switch2State = 0;

int pin11 = 4;
int pin11State = 0;
int pin12 = 5;
int pin12State = 0;

void setup() {
  pinMode(led1,OUTPUT);            // solenoid 1
  pinMode(solenoidPin1,OUTPUT);
  pinMode(led2,OUTPUT);            // solenoid 2, relief valve
  pinMode(solenoidPin2,OUTPUT);
  pinMode(led3,OUTPUT);            // solenoid 3
  pinMode(solenoidPin3,OUTPUT);
  pinMode(switch1,INPUT);
  pinMode(switch2,INPUT);

  pinMode(pin11,INPUT);            // D11 on printer
  pinMode(pin12,INPUT);            // D12 on printer

  // at start, only relief valve is open
  digitalWrite(led1,LOW);
  digitalWrite(solenoidPin1,LOW);
  digitalWrite(led2,HIGH);
  digitalWrite(solenoidPin2,HIGH);
  digitalWrite(led3,LOW);
  digitalWrite(solenoidPin3,LOW);
  Serial.begin(9600);
}
```

Figure 25 - Variable Definition and Initial Valve Setup Configuration

```
void loop() {
  switch1State = digitalRead(switch1);
  switch2State = digitalRead(switch2);
  pin11State = digitalRead(pin11);
  pin12State = digitalRead(pin12);

  Serial.println(pin11State);

  if (switch1State == 1){                // SOLENOID 1 ON
    digitalWrite(led1,HIGH);
    digitalWrite(solenoidPin1, HIGH);
    digitalWrite(led2,LOW);
    digitalWrite(solenoidPin2,LOW);
    digitalWrite(led3,LOW);
    digitalWrite(solenoidPin3,LOW);
  }
  else if (switch2State ==1){            // SOLENOID 3 ON
    digitalWrite(led1,LOW);
    digitalWrite(solenoidPin1, LOW);
    digitalWrite(led2,LOW);
    digitalWrite(solenoidPin2,LOW);
    digitalWrite(led3,HIGH);
    digitalWrite(solenoidPin3,HIGH);
  }
  else{                                  // SOLENOID 2 ON, RELIEF
    digitalWrite(led1,LOW);
    digitalWrite(solenoidPin1, LOW);
    digitalWrite(led2,HIGH);
    digitalWrite(solenoidPin2,HIGH);
    digitalWrite(led3,LOW);
    digitalWrite(solenoidPin3,LOW);
  }
}
```

Figure 26 - Valve Control Loop

3.2.8. Printing Flow Logic

The logic of the printer functioning with all these prior sections working together is shown in Figure 27. This figure depicts an example of turning on solenoid 1 and the processing associated with to depositing a bioink from syringe 1. First, in part a) the G-code command, M42 P11 S255 is sent to the printer from a connected computer or G-code file. This command instructs the printer to assign pin 11 the value 255. In part b) the printer sets pin 11 to 255 and the signal is received by the Arduino. After the signal is received, the Arduino commands solenoid 1 to open in part c). The final step, part d) is where the solenoid opens which results in bioink deposition. The functionality of 3D printing allows us to insert the M42 command at specific locations within the G-code file to allow for proper deposition of each bioink.

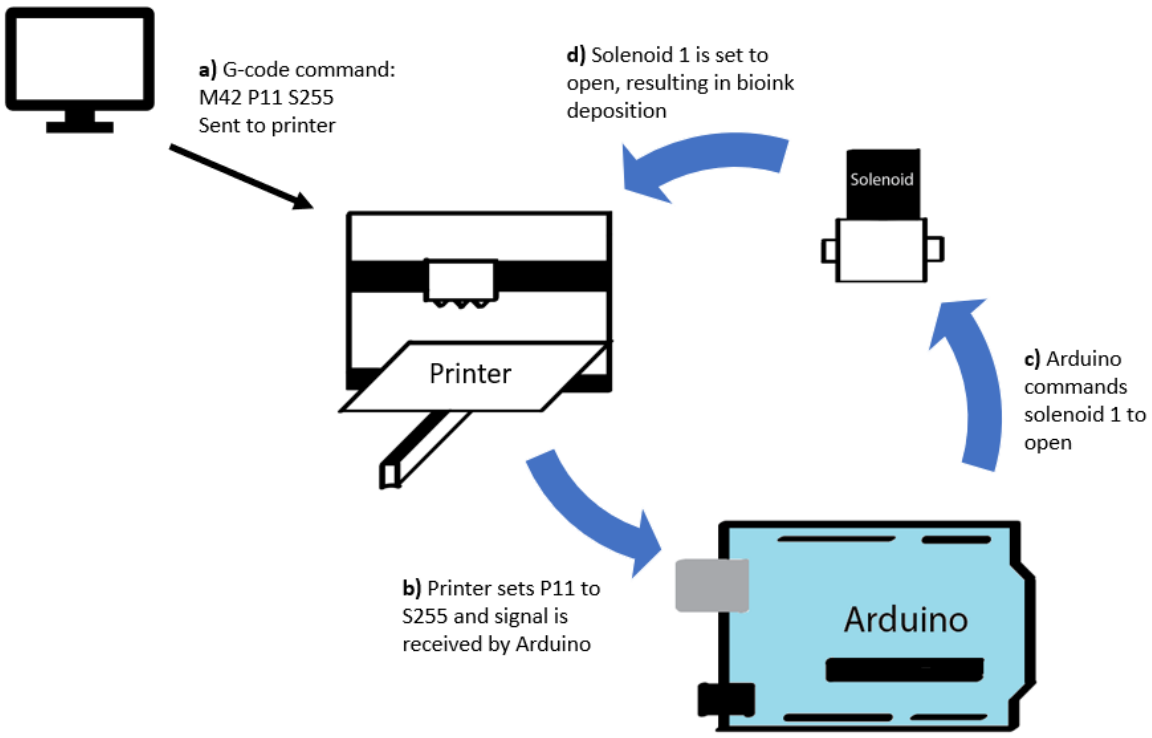

Figure 27 - Printing Flow Logic

3.2.9. Printing Setup Process

The process of setting up the system to printing is not a straightforward task. This is because there are multiple individual systems working together to achieve bioprinting. Shown below are the steps required to setup up the system for printing.

1. Plug in the power source to the printer and external 24-volt power unit.
2. Connect the printer motherboard to the computer.
3. Connect Repetier-Host from the computer to the printer.
4. Connect the solenoid control unit to the computer.
5. Manually input commands M42 P11 S0 and M42 P12 S0.
6. Turn on the external 12-volt power supply.
7. Turn on air supply to the solenoid control unit.
8. Ready to print.

3.3.Results

3.3.1. Triple Extruding 3D Bioprinter Setup

This triple extruding 3D bioprinter has many components that work together in order to achieve liquid deposition. The full setup of the 3D bioprinter is shown in Figure 28. On the far right of the image are the three solenoids, air supply, and 12-volt DC power supply. Inside the cardboard box on the right side is the Arduino microcontroller. The left half of the image displays the main printing platform.

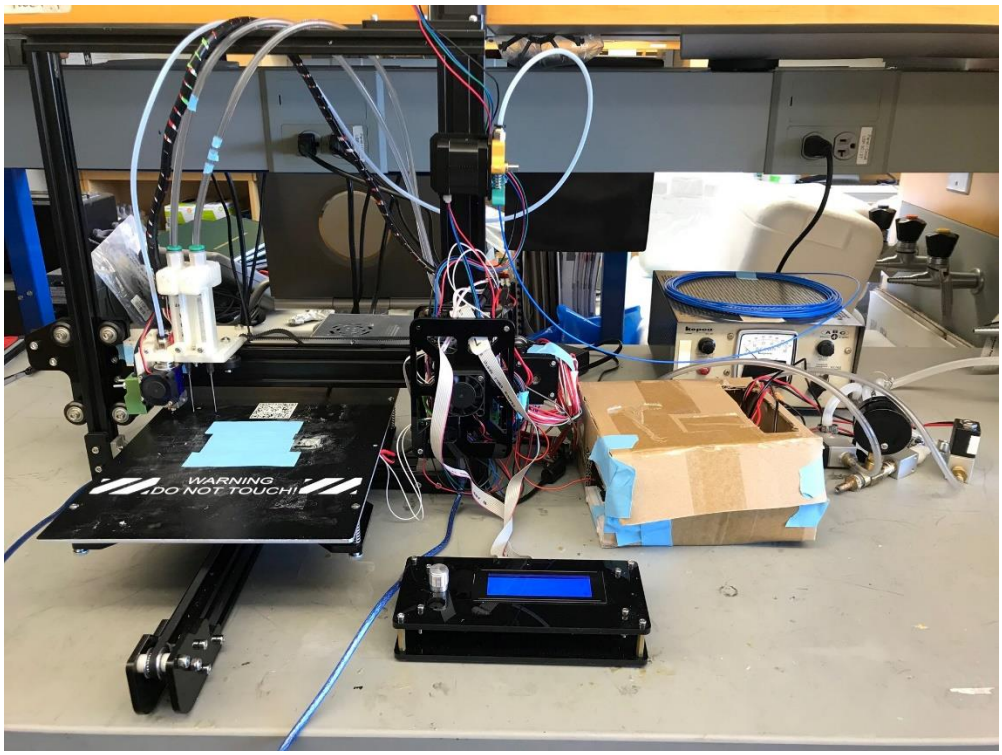

Figure 28 - Triple Head 3D Bioprinter Setup

3.3.2. Test Prints

In order to test the functionality of the printer, we printed a three-layered structure made of three different materials. The CAD representation and printed product are shown in Figure 29. In the CAD representation, the three layers are distinguished by the colors red, green, and blue. The red layer represents a thermoplastic, in this case PLA. The green and blue layers represent two different PEG based hydrogels. The final product shown on the right uses a blue PLA filament as the first layer, an orange hydrogel as the second layer, and a blue hydrogel as the third layer. This test print was repeated successfully and demonstrates that the printer's ability to construct products made of three different materials.

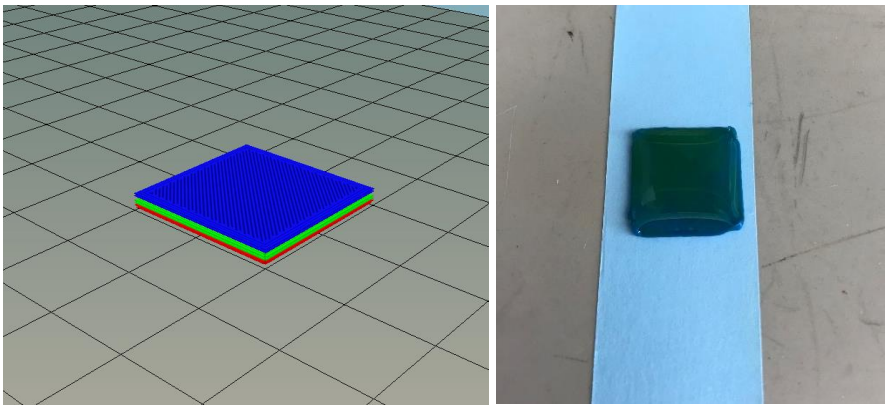

Figure 29 - Test Print, 3 layers

3.2.3. Discussion

By building upon our previous work, we have successfully built a pneumatic pressure driven triple head bioprinting system. We have shown that the printer can deposit a thermoplastic material alongside two bioinks. This printer however is still in developmental stages and requires additional work to make the system more user friendly and create higher quality prints.

Future work should include the addition of an ultraviolet light module for cross linking. This component will allow deposited bioinks to be crosslinked immediately after extrusion which would prevent the material losing its shape [17]. The print carriage should also be redesigned to make use of shorter syringe tip lengths. This is because, as stated in section 2.4, long syringe long syringe tips shear cells and reduce cell viability while printing. Similar to the study in chapter 2, the nozzle lengths used in our study were 38.1 mm. By using shorter syringe tip lengths, we can presumably increase cell viability [23].

Furthermore, the majority of our system requires manual inputs for complete setup. This process is defined in section 3.2.9 where the printing setup is described. This

process should be simplified to the point where the user only needs to press a button to power on the system and connect a computer to the printer. The current process requires seven steps to reach this point.

In addition, the incorporation of pressure regulators for both syringes would be a significant upgrade. This would allow different pressures to be distributed to each individual syringe. This would be important addition when using two bioinks of different viscosities. Currently the solenoids are connected to one air source which requires both liquids to be the same viscosity.

Although this printer is still in the developmental stage and additional funding is required to carry out these improvements, the cost of these additions should not exceed the price of commercially available 3D bioprinters which are listed at $8,750 and greater [17]. When analyzing current spending to create this printer, the total cost was $735. The base printer and additional mechanical components made up approximately 84% of the total cost. Additional electronic components made up 12% and the solenoid valves made up 4% of the total cost. The majority of the mechanical components were purchased as a DIY 3D printer kit in order to simplify the build process and provide a template to build on.

3.4. Conclusion

By building off a DIY 3D printer and leveraging the functionalities of 3D printing and an Arduino microcontroller, we developed a low-cost triple head 3D bioprinter that can deposit two bioinks and a thermoplastic to create multi-material structures. The core printing functionality of this printer has been established; however supplementary

functions still need development. Future work should aim to develop these functions along with further improving the core printing function.

CHAPTER 4: CONCLUSION

We have presented two methods for building two low-cost 3D bioprinters that are significantly cheaper than commercially available 3D bioprinters. The first being a 3D printable modification that was applied to a MakerBot Replicator Original Dual. By using this modification and a Python parsing program, we have demonstrated the ability to build a dual head 3D bioprinter that can construct complex tissue scaffolds. Furthermore, we characterized the quality of prints produced by this bioprinter along with the mechanical properties of constructed scaffolds. The second system is a pneumatic pressure driven triple head 3D bioprinter capable of depositing two bioinks and one thermoplastic material. The triple head 3D bioprinter is still in developmental stages however the core printing function works. In conclusion, we have shown the ability to build low cost 3d bioprinters that are capable of fabricating complex scaffolds made of different materials.

REFERENCES

1. Derakhshanfar, S. and e. al., *3D bioprinting for biomedical devices and tissue engineering: A review of recent trends and advances.* Bioactive Materials, 2018. **3**(2): p. 144-156.
2. Du, X., *3D Bio-Printing Review.* IOP Conference Series: Materials Science and Engineering. **301**(1).
3. Kang, H. and e. al., *A 3D bioprinting system to produce human-scale tissue constructs with structural integrity.* Nature Biotechnology, 2016. **34**: p. 312-319.
4. Liaw, C. and e. al., *Engineering 3D Hydrogels for Personalized In Vitro Human Tissue Models.* Advanced Healthcare Materials, 2018. **7**(4).
5. Knowlton, S. and e. al., *3D-printed microfluidic chips with patterned, cell-laden hydrogel constructs.* Biofabrication, 2016. **8**(2).
6. Jia, W. and e. al., *Direct 3D bioprinting of perfusable vascular constructs using a blend bioink.* Biomaterials, 2016. **106**: p. 56-58.
7. Chan, B.P. and K.W. Leong, *Scaffolding in tissue engineering: general approaches and tissue-specific considerations.* European Spine Journal, 2008. **4**: p. 467-479.
8. Wu, Z. and e. al., *Bioprinting three-dimensional cell-laden tissue constructs with controllable degradation.* Scientific Reports, 2016. **6**.
9. Lee, V. and G. Dai, *Three-dimensional bioprinting and tissue fabrication prospects for drug discovery and regenerative medicine.* Advanced Health Care Technologies, 2015. **2015:1**: p. 23-25.
10. Horva´th, L. and e. al., *Engineering an in vitro air-blood barrier by 3D bioprinting.* Scientific Reports, 2015(7974).
11. Duan, B., *State-of-the-Art Review of 3D Bioprinting for Cardiovascular Tissue Engineering.* Annals of Biomedical Engineering, 2017. **45**(1): p. 195-209.
12. Khoda, A., B. Ozbolat, and B. Koc, *Organ printing: computer-aided jet-based 3D tissue engineering.* 133, 2011: p. 011001.
13. Peppas, N.A. and e. al., *Hydrogels in Biology and Medicine: From Molecular Principles to Bionanotechnology.* Advanced Materials, 2006. **18**(11): p. 1345-1360.
14. Shahinpoor, M. and e. al., *Ionic polymer-metal composites (IPMCs) as biomimetic sensors, actuators and artificial muscles – a review.* Smart Materials and Structures, 1998. **7**(6): p. R15-R30.
15. Browe, D.P., et al., *Characterization and optimization of actuating poly(ethylene glycol) diacrylate/acrylic acid hydrogels as artificial muscles.* Polymer, 2017. **117**: p. 331-341.
16. Dababneh, A.B. and I. Ozbolat, *Bioprinting Technology: A Current State-of-the-Art Review.* Journal of Manufacturing Science and Engineering, 2014. **136**(061016-11).
17. Yenilmez, B. and e. al., *Development and characterization of a low-cost 3D bioprinter.* Bioprinting, 2019. **13**(e00044).
18. Murphy, S.V. and A. Atala, *3D bioprinting of tissues and organs.* Nature Biotechnology, 2014. **32**(8): p. 773-85.

19. Reid, J.A., et al., *Accessible bioprinting: adaptation of a low-cost 3D-printer for precise cell placement and stem cell differentiation.* International Society of Biofabrication, 2016. **8**(2).
20. Ozbolat, I. and H. M., *Current advances and future perspectives in extrusion-based bioprinting.* Biomaterials, 2015. **76**: p. 321-343.
21. Ozbolat, I. and Y. Yu, *Bioprinting towards Organ Fabrication: Challenges and Future Trends.* IEEE Trans. Biomed. Eng, 2013. **60(3)**: p. 691–699.
22. Hinton, T.J., *Three-dimensional printing of complex biological structures by freeform reversible embedding of suspended hydrogels.* Science Advances, 2015. **1**(9).
23. Faulkner-Jones, A., et al., *Bioprinting of human pluripotent stem cells and their directed differentiation into hepatocyte-like cells for the generation of mini-livers in 3D.* Biofabrication 2015 **7**(4): p. 044102.
24. "G-code." G. 06 Apr. 2019 <https://reprap.org/wiki/G-code>.